How Vision Is Impaired From Aging to Early and Intermediate Age-Related Macular Degeneration: Insights From ALSTAR2 Baseline

Cynthia Owsley[1], Thomas A. Swain[1,2], Gerald McGwin, Jr.[1,2], Mark E. Clark[1], Deepayan Kar[1], Jason N. Crosson[1], and Christine A. Curcio[1]

[1] Department of Ophthalmology & Visual Sciences, Heersink School of Medicine, University of Alabama at Birmingham, Birmingham, Alabama, USA
[2] Department of Epidemiology, School of Public Health, University of Alabama at Birmingham, Birmingham, Alabama, USA

Correspondence: Cynthia Owsley, Department of Ophthalmology & Visual Sciences, Heersink School of Medicine, University of Alabama at Birmingham, 1670 University Boulevard, Birmingham, AL 35294, USA.
e-mail: cynthiaowsley@uabmc.edu

Purpose: We hypothesize the first visual dysfunction in transitioning to early and intermediate age-related macular degeneration (AMD) is delayed rod-mediated dark adaptation (RMDA), owing to impaired photoreceptor sustenance from the circulation. This analysis from the Alabama Study on Early Age-related Macular Degeneration 2 provides insight on our framework's validity, comparing RMDA and other visual tests among older normal, early, and intermediate AMD eyes.

Methods: AMD disease severity was determined via fundus photos using the Age-Related Eye Disease Study nine-step system. Visual functions evaluated were RMDA 5°, acuity, contrast sensitivity (photopic, mesopic), and light sensitivity for a macular grid (scotopic, mesopic, photopic). Presence versus absence of subretinal drusenoid deposits (SDD) was identified through multimodal imaging.

Results: One eye from each of 481 persons (mean age, 72 years) was evaluated. All visual functions were significantly worse with increasing AMD disease severity. Using z-scores to standardize visual function measures across groups, the greatest difference in probability density functions between older normal and intermediate AMD was for RMDA. Early and intermediate AMD eyes with SDD present had longer rod intercept times than eyes with SDD absent. SDD absent eyes also exhibited delayed RMDA and wide probability density functions relative to normal eyes.

Conclusions: Among the visual functions evaluated, RMDA best discriminates among normal, early AMD, and intermediate AMD eyes. The Alabama Study on Early Age-related Macular Degeneration 2 will evaluate whether AMD's natural history confirms our hypothesis at the 3-year follow-up.

Translational Relevance: Results support a sequence of visual function impairments in aging and AMD, suggesting RMDA as a promising outcome for evaluating interventions in early disease.

Introduction

Age-related macular degeneration (AMD) is the leading cause of irreversible vision impairment in adults in the United States[1,2] and a prevalent cause of vision loss in adults worldwide.[3] AMD affects the photoreceptor support system, involving the choroid, Bruch's membrane, and retinal pigment epithelium (RPE), impacting retinoid resupply and leading to photoreceptor demise and vision loss.[4] Understanding what types of vision impairment occur in persons at risk for or diagnosed with AMD is useful for at least two reasons. First, the time course and severity of various types of vision impairment can reveal cues to the mechanisms of disease initiation that can inform theories and models of early AMD pathogenesis. Second, studies on visual dysfunction in AMD can
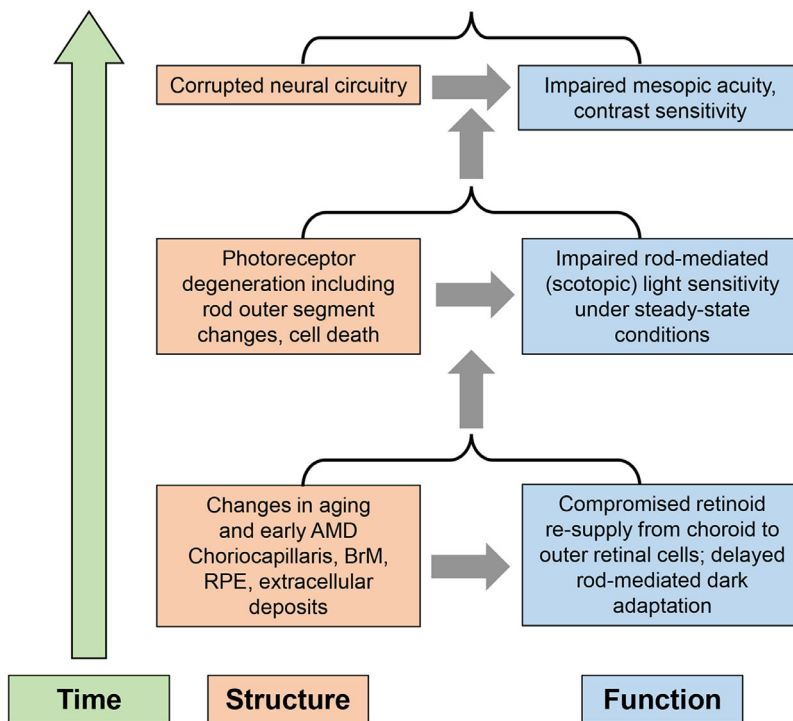
Figure 1. A conceptual framework for how visual deficits emerge over time during the natural history of aging transitioning to intermediate AMD. We hypothesize that the types of visual dysfunction that emerge will reflect structural changes in the retina over time. See text for details.

uncover candidate functional end points and outcomes in clinical interventions to slow or arrest AMD progression or prevent its onset.

Starting 30 years ago, several studies demonstrated the selective vulnerability of scotopic vision in aging and early AMD. Steady-state rod-mediated sensitivity was significantly impaired; in contrast, cone-mediated sensitivity was largely spared.[5–9] These findings were consistent with anatomic data from human donor eyes, demonstrating that rods in the macula degenerated and died during aging and early to intermediate AMD. Cones were relatively resilient, and they outlasted the rods by surviving into advanced disease.[10–12] In addition to changes in steady state sensitivity, aging impacts a dynamic aspect of scotopic function, in that the rate of rod-mediated dark adaptation (RMDA) slows markedly.[13] Compared with aging, RMDA delays are accentuated in early and intermediate AMD[9,14–20] and can be more severe in eyes with subretinal drusenoid deposits (SDD) (or reticular pseudodrusen).[15,16,21] Furthermore, the first functional biomarker identified for incident early AMD was delayed RMDA,[22] which was also associated with the presence of the two strongest risk alleles for AMD, *ARMS2* and *CFH*.[23]

The literature on visual dysfunction in early and intermediate AMD also suggests that other aspects of vision impairment under mesopic and photopic conditions occur in early and intermediate AMD (summarized here).[24,25] Interpreting these widespread reports of various visual deficits in AMD at various luminance adaptation levels would benefit from more data on natural history and severity of visual deficits during the transition from normal macular health to intermediate AMD.

Figure 1 presents a conceptual framework for how visual deficits emerge over time during the natural history of aging transitioning to intermediate AMD in the cone-dominated fovea and rod-dominated parafovea and perifovea. The bottom of the figure represents older adults who are in normal macular health yet exhibit small extracellular deposits (drusen, SDD) that impede the transfer of essential molecules from the circulation, including retinoids required by phototransduction.[26,27] Because of aging-related and early AMD changes in the choriocapillaris, Bruch's membrane, and the RPE,[28–33] the efficiency of the classic visual cycle becomes compromised. The visual cycle refers to the process of eliminating the products of light absorption from the outer segments, recycling of released retinoid to its original form

(11-*cis*-retinal), and regenerating the visual photopigment opsin. Measuring RMDA assesses the efficiency of this process.[26,27,34] We, thus, hypothesize that the earliest and most severe visual dysfunction to initially emerge in AMD is delayed RMDA. Because cones are also served by a second visual cycle (in Müller glia),[35,36] they are less vulnerable in aging and early and intermediate AMD to changes in the RPE, Bruch's membrane, and the choriocapillaris, as compared with rods. As early AMD progresses (middle of figure), rod outer segments shorten and degenerate, and cells die; we hypothesize that decreased steady-state scotopic sensitivity will then emerge. Finally, with further progression to the intermediate AMD stage (top of Fig. 1), retinal signal transmission between photoreceptors and bipolar cells and inner retina becomes corrupted owing to aberrant neural connectivity. By the time intermediate AMD emerges, we hypothesize that this corrupted circuitry will induce impairments in pattern vision, such as in mesopic acuity and contrast sensitivity.

We are currently conducting a longitudinal study (Alabama Study on Early Age-related Macular Degeneration 2 [ALSTAR2])[37] designed to evaluate this conceptual framework and associated hypotheses. The baseline, cross-sectional data from this study provide the opportunity to compare various types of visual function in normal older, early AMD, and intermediate AMD eyes. Comparing the differences in visual measures across disease severity in a cross-sectional manner can provide insight into the validity of the conceptual framework.

Methods

This study was approved by the Institutional Review Board of the University of Alabama at Birmingham. All participants provided written informed consent after the nature and purpose of the study were explained. Conduct of the study followed the tenets of the Declaration of Helsinki.

Baseline data from ALSTAR2 are used in this analysis. ALSTAR2 is a prospective cohort study on normal aging and early and intermediate AMD whose purpose is to validate with visual function testing retinal imaging characteristics in these conditions (Clinicaltrials.gov identifier NCT04112667, October 7, 2019).[37]

Participants aged 60 years or older were recruited from the Callahan Eye Hospital Clinics, the clinical service of the University of Alabama at Birmingham Department of Ophthalmology and Visual Sciences. Our focus was on forming three participant groups—those with early AMD and intermediate AMD and those in normal macular health. The clinic's electronic health record was used to search for patients with early or intermediate AMD using *International Classification of Diseases*, 10th edition, codes for these conditions (H35.30*; H35.31*; H35.36*). One of the investigators (C.O.) screened the charts to ensure that participants met the eligibility criteria. Exclusion criteria were (1) any eye condition or disease in either eye (other than early cataract) in the medical record that can impair vision, including diabetic retinopathy, glaucoma, ocular hypertension, a history of retinal diseases (e.g., retinal vein occlusion, retinal degeneration), optic neuritis, corneal disease, previous ocular trauma or surgery, or a refractive error of 6 or more diopters; (2) neurological conditions that can impair vision or judgment including multiple sclerosis, Parkinson's disease, stroke, Alzheimer's disease, seizure disorders, brain tumor, or traumatic brain injury; (3) psychiatric disorders that could impair the ability to follow directions, answer questions about health and functioning, or provide informed consent; (4) diabetes; and (5) any medical condition that causes liver disease, significant frailty, or was thought to be terminal. Persons in normal macular health were recruited with the same eligibility criteria, except that they did not have *International Classification of Diseases*, 10th edition, codes indicative of AMD. Letters were sent to potential participants, and the study coordinator followed up with a phone call to determine interest.

One eye was tested in each participant. The eye selected for testing was the eye with better acuity. If the eyes had the same acuity, then an eye was selected randomly. Classification into the three groups was based on a trained grader's evaluation of three-field, color fundus photographs taken with a digital camera (450+; Carl Zeiss Meditec, Dublin CA) after dilation with 1% tropicamide and 2.5% phenylephrine hydrochloride. The Age-Related Eye Disease Study (AREDS) nine-step classification system[38] was used by a trained grader to identify the presence and severity of AMD in the eye, and group membership was determined on this basis. Group definitions were as follows: those eyes with normal macular health had AREDS grade 1, early AMD had grades 2 to 4, and intermediate AMD had grades 5 to 8. The grader was masked to all other participant characteristics. We also used the Beckman classification system[39] for identifying presence and severity of AMD. Normal aging was defined as grades 1 to 2, early AMD as grade 3, and intermediate AMD as grade 4.

Demographic information for birthdate, gender, and race/ethnicity was obtained through self-administered questionnaire. Visual acuity and contrast sensitivity, both established tests of pattern vision,

were tested under photopic and mesopic background conditions. Best-corrected letter visual acuity under photopic conditions (100 cd/m^2) was assessed with the Electronic Visual Acuity tester (JAEB Center, Tampa FL)[40] and expressed as logarithm$_{10}$ of the minimum angle of resolution. Acuity was also tested under mesopic conditions while the participant viewed the display through a 2.0 log unit neutral density filter (mesopic condition, 1 cd/m^2).[41] Photopic contrast sensitivity for letters was tested (100 cd/m^2) with the Mars chart (Mars Perceptrix, Chappaqua NY),[42] and scored letter by letter defined as log contrast sensitivity. This test was also repeated under mesopic conditions using the 2.0 log unit neutral density filter (as described for acuity).

Steady-state light sensitivity for the same grid of perimetric target locations in the macula were tested under photopic, mesopic, and scotopic conditions ("steady-state" means that eyes were adapted to the background luminance of testing before testing began). The nontested eye was covered with an eye patch. Targets in all perimetry tests were 0.43° in diameter (Goldmann size III). The target grid had 21 test locations at 0° (fovea) and at 5°, 10°, and 12° in all quadrants for mesopic and photopic perimetry (described previously).[37] For scotopic perimetry, the grid was identical, except for the absence of a test spot in the rod-free fovea. For scotopic testing we used the S-MAIA microperimeter and a cyan (505 nm) target (iCare, Vantaa, Finland) (background level 0 cd/m^2). Participants were adapted to darkness for 30 minutes before scotopic testing. The S-MAIA was also used for mesopic testing with white targets (background level of 1.27 cd/m^2). S-MAIA measurements were done under dilation. Participants with high fixation errors (>30% for the S-MAIA) were removed from mesopic and scotopic light sensitivity analyses. A microperimeter for photopic testing was not available, so a Humphrey Field Analyzer 3 (Carl Zeiss Meditec) was used (background level of 10 cd/m^2). Participants with photopic testing fixation errors, false positives, or false negatives of 33% or more were excluded from the analysis of photopic light sensitivity.

RMDA was assessed with the AdaptDx (MaculLogix, Harrisburg PA). Testing occurred in a dark, light-tight room after dilation. Dark adaptation was measured with targets at 5° on the superior vertical meridian of the retina, because rod loss is proportionally maximal in aging and AMD at 5°.[10,11] The procedure began with a photo-bleach exposure to a 6° flash centered at the test target location (50 ms duration, 58,000 scotopic cd/m^2 s intensity)[43] while the participant focused on the fixation light at a distance of 30 cm. Threshold measurement (three-down/one-up

threshold strategy) for a 2° diameter, 500 nm circular target began 15 seconds after bleach offset. The participant was instructed to maintain fixation and press a button when the flashing target first became visible. Log thresholds were expressed as sensitivity in decibel units as a function of time since bleach offset. Threshold measurement continued at 30-second intervals until the rod intercept time (RIT) was reached. The RIT is the duration in minutes required for sensitivity to recover to a criterion value of 5.0×10^{-3} scotopic cd/m^2,[22,44] located in the latter one-half of the second component of rod-mediated recovery.[26,45] If the RIT was not reached, the threshold measurement procedure stopped at 45 minutes. Participants with fixation errors of more than 30% were excluded from the analysis.

Multimodal Image Capture and Analysis

The presence of SDD, also known as reticular pseudodrusen,[30] was identified using multimodal imaging in two steps. The screening step included verifying SDD presence using near infrared reflectance (NIR) and en face optical coherence tomography (OCT) (Supplementary Fig. S1). In NIR imaging, SDD lesions had to be visible as either solid or annular hyporeflective lesions in a distinct punctate pattern. In en face OCT, the SDD had to be visible as a patchy hyperreflective pattern or solitary hyperreflective lesions surrounded by a hyporeflective annulus. Once the SDD was visible on either NIR or en face OCT, at least 5 definite drusenoid accumulations above the RPE in more than 1 B-scan on cross-sectional OCT were required for confirming SDD presence.

NIR and OCT B-scans were sourced from spectral domain OCT volumes captured for each participant (Spectralis HRA + OCT; Heidelberg Engineering, Heidelberg, Germany; λ = 870 nm; scan depth, 1.9 mm; axial resolution, 3.5 μm per pixel in tissue; lateral resolution, 14 μm per pixel in tissue), with Automatic Real-Time averaging of more than 9, and quality (signal-to-noise) of 20 to 47 dB. B-scans (*n* = 121 scans, spacing = 60 μm) were horizontally oriented and centered over the fovea in a 30° × 25° (8.6 × 7.2 mm) scan pattern. En face OCT was sourced from volumes captured using the OCT-Angiography Module of Spectralis HEYEX software (version 6.10.6.0). Two 15° x 15° (4.4 × 4.4 mm) volumes of the fovea (0°) and superior perifovea (12°) comprised 384 B-scans with 11 μm spacing. The use of two en face OCT scans with approximately a 14% overlap in area allowed a combined sampling of up to 18° superiorly from the foveal center. En face OCT slabs were generated by setting the top boundary at the external limiting membrane band and the lower

boundary at the interdigitation zone band (called PR2 in HEYEX).

SDD presence was assessed by a grader masked to all visual functional characteristics. A second grader, also masked to visual function, assessed a randomly selected 14% subsample of study eyes. Agreement with the first grader on the presence of SDD was strong (Cohen's $\kappa = 0.89$; 95% confidence interval 0.77–1.0).

Statistical Analyses

Participant demographics and visual functions were summarized using means and standard deviations for continuous data and number and percent for categorical data. Differences in age by AMD status were tested with a one-way analysis of variance. Analysis of covariance with pairwise comparisons was used to test for differences in continuous visual functions by AMD status adjusting for age. The same method was used to compare RIT by SDD presence versus absence. Because of differences in units and distributions for the various visual function tests, comparing the differences between the groups for the function measures would not be meaningful. Therefore, to facilitate these comparisons, we considered all three groups as a single sample to compute z-scores for each vision measure. In computing z-scores, the mean value for a given measure was subtracted from the individual participant's value and then divided by the standard deviation. For each vision measure, the calculated z-scores will have a mean of zero and a standard deviation of 1. All z-scores were standardized so that positive z-scores denote worse vision, and negative z-scores denote better vision. The scales for contrast sensitivity and light sensitivity measures were, thus, reversed so that higher z-scores represent worse visual function, as they do for RMDA and visual acuity. For each vision measure, probability density functions (PDFs)[46] for the z-scores were plotted for each group to illustrate differences in the distributions by AMD status. PDFs are statistical functions that describe the likelihood of obtaining possible values that a continuous variable, such as visual function, can take. Because continuous variables, such as z-scores, can take on an infinite number of values, PDFs are used to facilitate the visualization of the probability that certain values are observed, akin to a frequency distribution for a categorical variable. The area under each density curve sums to 1. PDFs provide information about the likelihood of observing visual function measurements (i.e., the density), as well as their spread. All analysis was done using SAS version 9.4 (SAS Institute, Cary, NC). Density distribution curves were generated using R version 4.1.1 (The R Foundation, Vienna, Austria).

Results

The baseline data were collected between October 2019 and September 2021, which included a 4-month stoppage in enrollment owing to the coronavirus

Table 1. Demographic Characteristics of the Sample (481 Eyes From 481 Persons)

	Overall Sample (n = 481)		Normal Macular Health (n = 239)		Early AMD (n = 139)		Intermediate AMD (n = 103)	
Mean Age, Years	71.8 ± 5.9		70.8 ± 5.6		71.3 ± 6.1		74.5 ± 5.6	
	n	%	n	%	n	%	n	%
Age, years								
60–69	170	35.3	99	41.4	52	37.4	19	18.5
70–79	263	54.7	125	52.3	74	53.2	64	62.1
80–89	47	9.8	15	6.3	13	9.4	19	18.5
90–99	1	0.2	0	0.0	0	0.0	1	1.0
Sex								
Female	288	59.9	154	64.4	78	56.1	56	54.4
Male	193	40.1	85	35.6	61	43.9	47	45.6
Race/ethnicity								
White[a]	436	90.6	212	88.7	125	89.9	99	96.1
Black	40	8.3	25	10.5	11	7.9	4	3.9
Other[b]	5	1.0	2	0.8	3	2.2	0	0.0

[a]Of non-Hispanic origin.
[b]Two participants were American Indian and three were Asian or Pacific Islander.

Table 2. Visual Function Mean and Standard Deviations and Age-Adjusted Comparisons by AMD Severity For All Eyes (*N* = 481)

| Visual Function	Normal Macular Health (*n* = 239)[a] Mean ± SD	Early AMD (*n* = 139)[a] Mean ± SD	Intermediate AMD (*n* = 103)[a] Mean ± SD	*P* Values			
				Overall	Normal vs. Early AMD	Normal vs. Intermediate AMD	Early vs. Intermediate AMD
RMDA 5°, RIT in minutes	12.1 ± 5.4	15.3 ± 9.0	29.2 ± 12.4	<0.0001	0.0005	<0.0001	<0.0001
Photopic acuity, logMAR	−0.03 ± 0.09	−0.03 ± 0.11	0.02 ± 0.11	0.0027	0.6195	0.0023	0.0014
Mesopic acuity, logMAR	0.20 ± 0.11	0.20 ± 0.13	0.30 ± 0.17	<0.0001	0.8348	<0.0001	<0.0001
Photopic contrast sensitivity, log sensitivity	1.61 ± 0.11	1.60 ± 0.12	1.53 ± 0.14	<0.0001	0.2858	<0.0001	0.0002
Mesopic contrast sensitivity, log sensitivity	1.21 ± 0.20	1.19 ± 0.17	1.08 ± 0.18	<0.0001	0.5494	<0.0001	0.0003
Photopic light sensitivity, dB[4]	29.3 ± 2.1	29.6 ± 1.7	28.4 ± 2.2	0.0130	0.2347	0.0317	0.0035
Mesopic light sensitivity, dB	23.1 ± 2.0	23.2 ± 1.8	21.8 ± 2.8	0.0017	0.4591	0.0023	0.0006
Scotopic light sensitivity, dB	19.2 ± 1.6	18.9 ± 1.9	17.4 ± 3.5	<0.0001	0.3434	<0.0001	<0.0001
Scotopic light sensitivity at 5°	19.2 ± 1.6	19.0 ± 1.8	17.4 ± 3.5	<0.0001	0.7477	<0.0001	<0.0001

[a]The *n* is reduced to 193 for mesopic contrast sensitivity among normals. The *n* is reduced for normals, early, and intermediate AMD respectively as follows: photopic light sensitivity (209, 122, 97), mesopic light sensitivity (197, 124, 83), and scotopic light sensitivity (220, 131, 93). For the scotopic light sensitivity at 5° RMDA test spot, the *n* is 219 for normals, 131 for early AMD, and 88 for intermediate AMD.

disease 2019 pandemic (March–June 2020). A follow-up visit will occur 3 years after enrollment, beginning in fall 2022.

Table 1 describes the demographic characteristics of the 481 study participants. Those with intermediate AMD were on average approximately 4 years older than those with normal macular health and early AMD (*P* < 0.0001). Participants were slightly more likely to be women than men; most participants were non-Hispanic Whites.

The means and standard deviations of the visual function tests stratified by AMD status are shown in Table 2. When comparing normal with intermediate AMD and early AMD with intermediate AMD, all visual tests were significantly worse in intermediate AMD. The only visual function significantly worse in early AMD as compared with older normal eyes was RMDA.

Figure 2 shows individual eye data for the RIT in each group comparing SDD present versus SDD
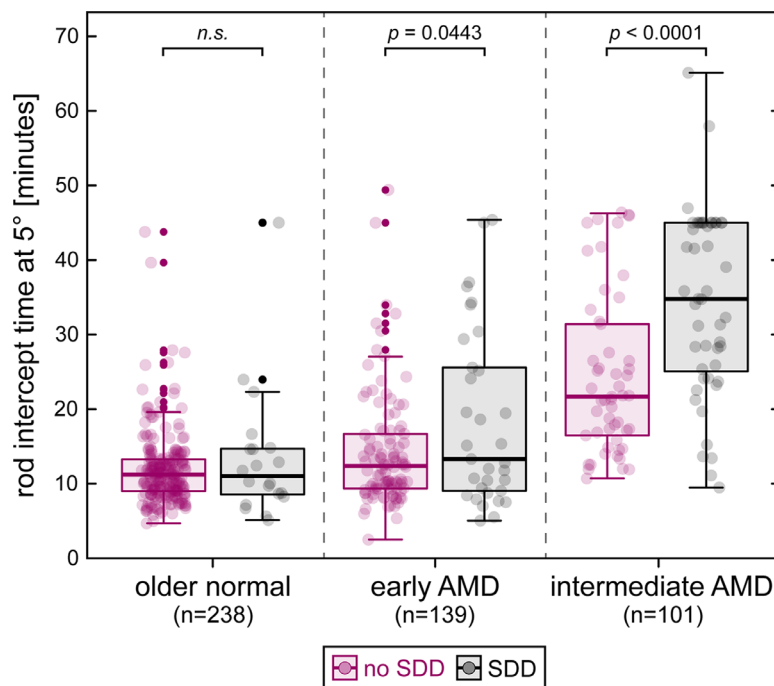
Figure 2. RIT stratified by disease severity and SDD absence versus SDD presence. Circles are data points from individual eyes. Box-and-whisker plots represent median and interquartile ranges. Early and intermediate AMD eyes with SDD present had longer RITs than eyes with SDD absent. Yet in these groups, SDD absent eyes also exhibited delayed RMDA. SDD grading was based on NIR as well as en face and B-scan OCT multimodal imaging (illustrated in Supplementary Figure S1). AMD severity groups are assigned based on color fundus photography grading (AREDS nine-step).
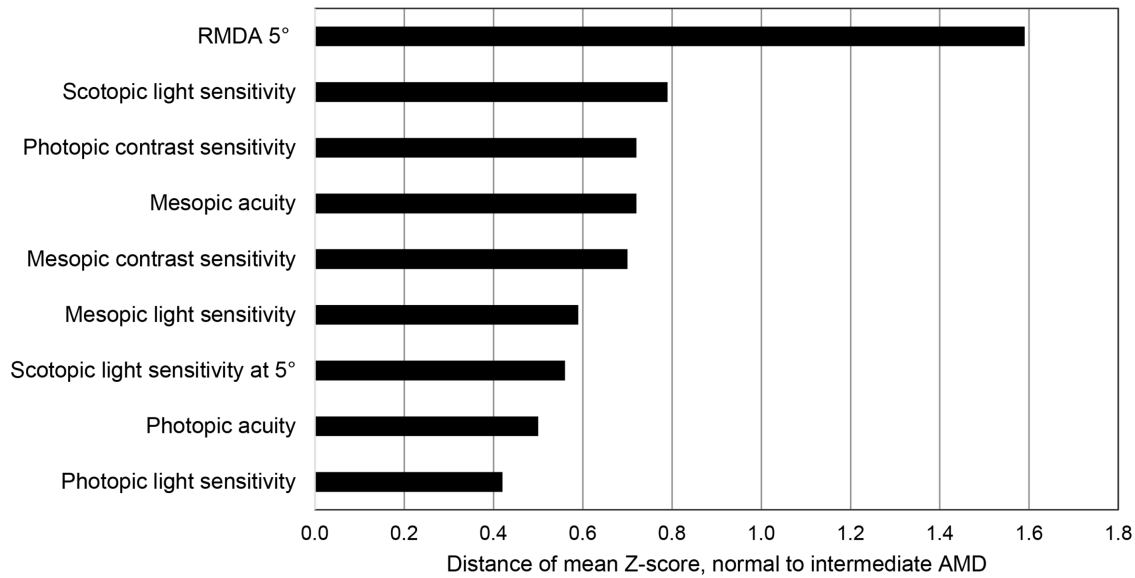
Figure 3. The difference between z-scores in normal aging and intermediate AMD. RMDA at 5° eccentricity (RMDA 5°) separates AMD diagnostic groups per the z-score difference better than other visual functions. The distances of mean Z-scores for each visual function (from Supplementary Table S2) are plotted in descending order for the 481 eyes. Photopic acuity and light sensitivity are the least likely to separate normal aging from intermediate AMD.

absent eyes. There is no difference in older normal eyes comparing SDD present and SDD absent. SDD eyes in early and intermediate AMD eyes had a longer RIT on average when compared with SDD absent eyes. Note the large overlap for RIT between the SDD present and SDD absent eyes in the early and intermediate AMD groups. As summarized in Supplementary Table S1, eyes with SDD constituted 8.4% of the normal group, 23.7% of the early AMD group, and 43.7% of the intermediate AMD group, or 21.1% of the total cohort.

The data for each visual function were expressed as z-scores based on the overall distribution of scores across all groups (normal macular health, early AMD, intermediate AMD), and then summarized for each group. Figure 3 shows the z-score difference from normal to intermediate AMD eyes. These data are shown in tabular form in Supplementary Table S2. The largest difference in function by AMD status was for RMDA at 5°, going from a mean of –0.43 in normal eyes to a mean of 1.16 in intermediate AMD eyes, with a z-score difference of 1.59. All z-score differences for other visual functions were much smaller, being one-half or less of the range for RMDA at 5°. For example, the next highest z-score difference for scotopic light sensitivity was 0.79 as compared with 1.59 for RMDA.

In Figure 3 (also in Supplementary Table S2) we examined the z-score difference for scotopic sensitivity specifically measured at 5°, which is the location of the RMDA test target. The rationale for this analysis is that previous work suggests that scotopic sensitivity is most impaired in early and intermediate AMD closer to the fovea than at more distant eccentricities[47]; thus, one might expect scotopic sensitivity at 5° to reveal more impairment in early and intermediate AMD than the mean scotopic sensitivity across a 20-target macular grid. However, the z-score difference for scotopic sensitivity at 5° was considerably smaller (0.56) than for RMDA at 5° (1.59). In addition, the z-score difference for scotopic sensitivity at 5° is also smaller than the average scotopic sensitivity z-score difference for the entire macular grid (0.76).

Figure 4 displays the z-score PDFs for all visual functions stratified by AMD status. Compared with other visual functions, the PDF for RMDA shows the widest range of values across all three groups (as indicated in Fig. 3 and Supplementary Table S2). The RMDA z-scores for intermediate AMD eyes are clearly skewed right to worse vision with the majority of scores being above 0 standard deviations, indicating that eyes with intermediate AMD have the greatest density of RMDA worse than the mean (0) (see blue area). This observation should be contrasted with the z-score density functions for all the other visual functions where there is extensive overlap in PDF among the three groups. A z-score density above 0 standard deviations for the other visual functions was much lower compared with RMDA, with the other groups having only a slight representation for intermediate AMD (sliver of blue in Fig. 4). The RMDA z-scores for normal and early AMD eyes are densest
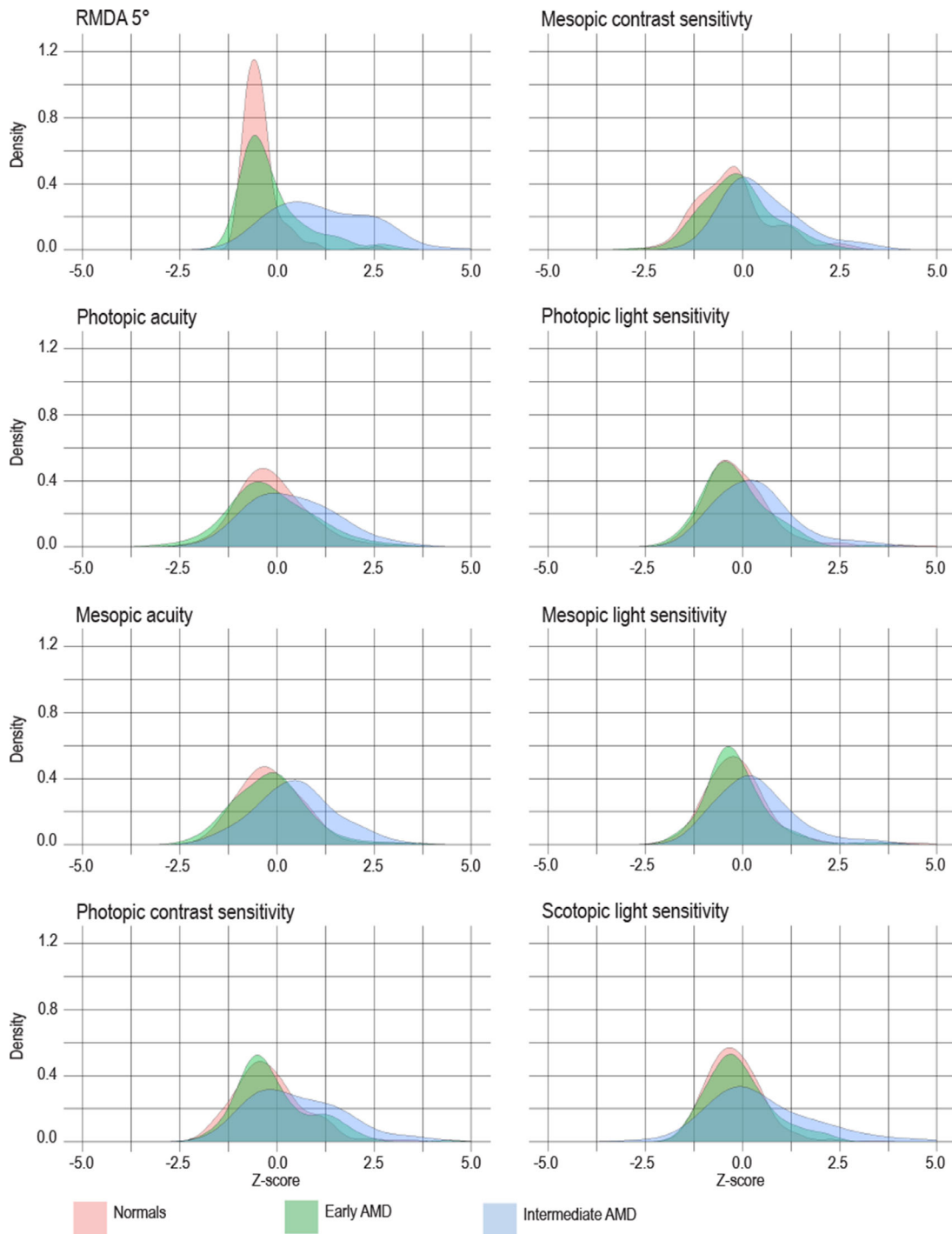
Figure 4. Z-score PDFs plotted for all visual functions (using the AREDS nine-step system). Each group is plotted separately: normal aging, pink; early AMD, green; and intermediate AMD, blue. PDFs are statistical functions describing the likelihood of obtaining possible values that a continuous variable can take (in this case, visual function). PDFs facilitate the visualization of the probability that certain variables are observed. The area under each density curve is 1. The abscissa is the z-score, and the ordinate is density. Higher z-scores correspond with worse vision, and lower z-scores correspond with better vision. To facilitate comparisons among visual function tests, the scales for contrast sensitivity and light sensitivity measures were reversed so they can be compared with RMDA and visual acuity. Compared with other visual functions, the PDF for RMDA shows the widest range of values across all three groups. RMDA z-scores for intermediate AMD eyes are clearly skewed right to worse vision with most scores being above 0 standard deviations (see blue area). This indicates that eyes with intermediate AMD have the greatest density of RMDA worse than the mean (0). This should be contrasted with the z-score density functions for all the other visual functions where there is extensive PDF overlap among the three groups. See text in Results for further comments.
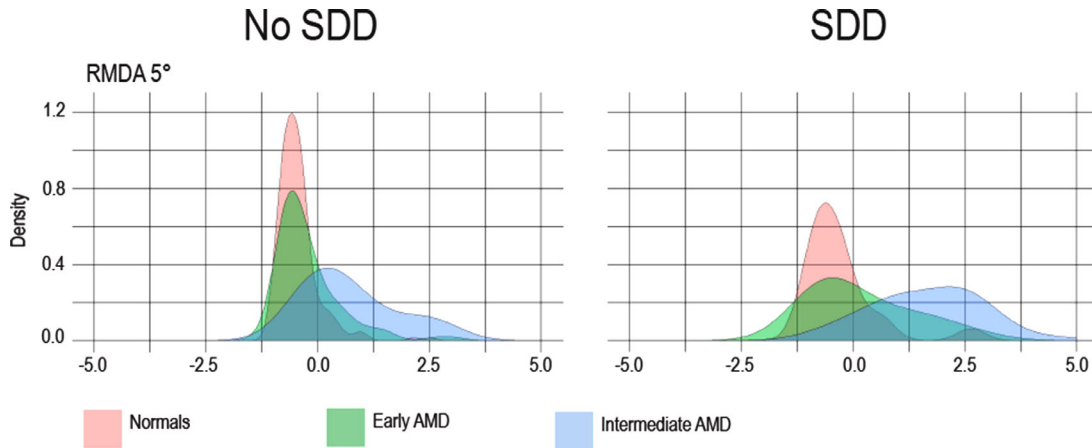
Figure 5. Z-score PDFs plotted for RMDA (using the AREDS nine-step system) stratified by SDD absence and presence. Each group (normal aging, early AMD, intermediate AMD) is plotted separately: normal aging, pink; and early AMD, green. Note that the SDD present density function for intermediate AMD has a greater density and more rightward distribution to higher RIT than for SDD absent (see blue area). However, the density function for SDD absent for intermediate AMD still maintains a large blue density to the right as compared with other visual functions in Figure 4.

between –1.25 and 0 z-scores, indicating better vision. The RMDA density of normal eyes is much higher than for early AMD. The density distributions of the other visual functions are very similar for normal eyes and early AMD eyes. Supplementary Figure S2 used the Beckman classification to define the presence and severity of AMD; the results are very similar to results using the AREDS nine-step definitions (Fig. 4).

We also compared PDFs for scotopic sensitivity and RMDA, both at 5° (Supplementary Fig. S3). The PDF for scotopic sensitivity had considerable overlap between the three groups, unlike the PDF for RMDA at the identical location, where the groups were well-differentiated. This separation was particularly noticeable for intermediate AMD, which has a large blue area in Supplementary Figure S3.

We compared the PDFs for RMDA for eyes with SDD absent to eyes with SDD present (Fig. 5). Although the SDD present density function for intermediate AMD is larger and positioned further to the right of SDD absent (i.e., slower RMDA, see blue area), the density function for SDD absent for intermediate AMD still maintains a wide blue density to the right, especially as compared with other visual functions in Figure 4.

Discussion

This proposed conceptual framework hypothesizes that the earliest visual dysfunction to emerge in AMD is delayed RMDA. Delayed RMDA is the most severely impacted visual function, until the well-documented loss of foveal acuity in advanced disease. This hypothesis could not be tested explicitly in the current analysis owing to the cross-sectional nature of the data. However, this cross-sectional design was appropriate for comparing a variety of visual functions under various background adaptation levels among older adults in normal macular health and with early and intermediate AMD. And by using this approach, we could gain insight into the natural history of visual dysfunction in AMD. Using z-scores to standardize vision measures and considering all groups together, the greatest difference between visual function in normal and intermediate AMD eyes was for RMDA, with all other visual functions displaying a difference that was only 26% to 51% of this difference for RMDA. The second largest difference between normal older eyes and intermediate AMD eyes was for average scotopic sensitivity across the 20-target macular grid, at only one-half of the difference for RMDA. The z-score density distributions stratified by disease severity indicated that the largest density of scores above 0 standard deviations for intermediate AMD eyes by far was for RMDA. For all other visual functions, the three groups had similar z-score density distributions, displaying considerable overlap among the groups. Even though scotopic sensitivity is most impaired close to the fovea,[47] scotopic sensitivity at 5° displayed a lower z-score difference across groups than did average scotopic sensitivity throughout the macula.

Eyes containing SDD are known to have markedly delayed RMDA.[15,16,21] In the ALSTAR2 baseline

cohort, eyes with SDD present had longer RITs on average than for eyes with no SDD in early and intermediate AMD. However, the impact of SDD on RIT does not account for our overall results, because eyes with SDD absent still had a delayed RMDA (see Fig. 2 and Supplementary Figure S2). To assess SDD presence, we built on prior work,[48,49] demonstrating the merit of en face OCT for SDD evaluation. We added novelty by leveraging the faster scan speed and greater B-scan density of OCTA to achieve reproducibly interpretable en face images that were verified as SDD by cross-sectional OCT in this large cohort. Further, our use of two overlapping OCT volumes extended our SDD evaluation area further into superior near-peripheral retina[50] (18° or approximately 5.1 mm eccentricity), into the region of high rod abundance where SDD first appear.[51] Our observed frequencies of 8.4%, 23.7%, and 47.5% in normal, early AMD, and intermediate AMD, respectively, are higher than that reported for other cohorts of varying size using cross-sectional OCT (as summarized by Wu et al.[52]) and lower than we reported for ALSTAR1, enrolled from the same clinic, using a different multimodal imaging strategy and less stringent criteria.[53] Wu et al.[52] suggested that, in cohorts assessed with cross-sectional OCT, in a smaller evaluation area than used in the current study, SDD is detected in 30% of individuals with intermediate AMD. Our data are not inconsistent with Wu et al.'s conclusion, given the differences in the study designs.

Although our data do not represent the natural history of within-subject changes, the results imply that RMDA may be the most useful functional end point for examining interventions targeted at arresting early and intermediate AMD progression, given the wide differences in RMDA from normal aging to intermediate AMD. We have previously shown that delayed RMDA in normal older eyes doubles the risk for incident AMD 3 years later,[22] whereas no such associations were noted for impairments in visual acuity, contrast sensitivity, and photopic light sensitivity.[54] ALSTAR2 has a 3-year follow-up visit beginning in late 2022, and thus a longitudinal evaluation of visual function during AMD's natural history will provide a direct evaluation of our hypothesis.

Guymer et al.[18] recently compared older control eyes (*n* = 23) with those with intermediate AMD (*n* = 25) identified through multimodal imaging with respect to RMDA (using RIT), scotopic and mesopic sensitivity, and photopic and mesopic acuity. These authors also used z-scores to standardize each visual function; however, their approach was different than ours. They used the normal group as the z-score reference. For each individual case in the intermediate AMD group,

they added this case to the normal group, and then computed the z-score for that case. This approach resulted in a mean of zero for older normals, which was then compared with the average z-scores of all the intermediate AMD cases. They found that the largest z-score was for RMDA (which they assessed at 4°). Their approach differs from ours in that we computed z-scores based on the three combined groups and then plotted the PDF to examine the density for various visual functions. Our rationale was that a proportion of eyes with normal fundi have delayed RMDA. However, our results and those of Guymer et al.[18] converge in agreeing that RMDA exhibits distributional characteristics that support use as an outcome or end point.

The strengths of our approach include a very large sample (*N* = 481) for studying visual function in all three groups, the inclusion of an early AMD group allowing for a continuum of disease from normal macular health to intermediate AMD, and a novel multimodal imaging method for ascertaining SDD presence. A limitation is that a direct assessment of the natural history of visual functional changes must await the ALSTAR2 follow-up to be started in October 2022.

A criticism of using RMDA testing as an outcome measure in AMD trials is test duration that, depending on the stimulus conditions and AMD severity, can range from approximately 8 to more than 40 minutes. Although RMDA testing is not brief (such as in letter visual acuity or contrast sensitivity testing), it is important to recognize the participant burden and duration of testing within the context of other functional outcome measures in retinal disease trials. In inherited retinal degeneration research, electroretinograms are often conducted, and, more recently, multiluminance mobility testing has been incorporated into gene therapy trials.[55] In these tests, the process of setup and testing is lengthy. Another criticism of RMDA testing is that some older persons cannot perform the RMDA test owing to frequent fixation errors. In the baseline visit of ALSTAR2, where the staff were well-trained to perform RMDA testing, 92% of all participants performed the protocol with less than 30% fixation errors, considered a threshold for frequent errors. As Guymer et al. pointed out,[18] the value in RMDA testing may outweigh its clinical difficulty, given that "no number of noninformative tests . . . will deliver the same informative data."

In summary, our results imply that there is a sequence of different types of visual function impairments as normal aging unfolds into early and intermediate AMD, which may follow the structural changes in the retina and choroid during AMD's natural history. The largest changes in the distribution between visual functions among normal older eyes and those with

early and intermediate AMD are delayed RMDA. Although these changes are stronger for early and intermediate eyes with SDD, they are also observed in eyes without SDD. Thus, this work encourages the notion that the most sensitive end point for evaluating interventions to arrest early AMD progression may be RMDA. This will be evaluated longitudinally in ALSTAR2.

Acknowledgments

Disclosure: **C. Owsley**, is an inventor on the device used to measure dark adaptation in this study (P); **T.A. Swain**, None; **G. McGwin**, None; **M.E. Clark**, None; **D. Kar**, None; **J.N. Crosson**, None; **C.A. Curcio**, receives research support from Genentech/Hoffman LaRoche and Regeneron, and consults for Apellis and Boehringer Ingelheim, all outside this work (F, C)

References

1. Klein R, Chou C-F, Klein BEK, Zhang X, Meuer SM, Saaddine J. Prevalence of age-related macular degeneration in the US population. *Arch Ophthalmol.* 2011;129:75–80.
2. The Eye Diseases Prevalence Research Group. Prevalence of age-related macular degeneration in the United States. *Arch Ophthalmol.* 2004;122:564–572.
3. World H Health Organization. Blindness and vision impairment. Available at: https://www.who.int/news-room/fact-sheets/detail/blindness-and-visual-impairment. Published 2021. Accessed November 8, 2021.
4. Fritsche LG, Fariss RN, Stambolian D, Abecasis G, Curcio CA, Swaroop A. Age-related macular degeneration: genetics and biology coming together. *Annu Rev Genomics Hum Genet.* 2014;15:151–171.
5. Chen JC, Fitzke FW, Pauleikhoff D, Bird AC. Functional loss in age-related Bruch's membrane change with choroidal perfusion defect. *Invest Ophthalmol Vis Sci.* 1992;33(2):334–340.
6. Steinmetz RL, Haimovici R, Jubb C, Fitzke FW, Bird AC. Symptomatic abnormalities of dark adaptation in patients with age-related Bruch's membrane change. *Br J Ophthalmol.* 1993;77:549–554.
7. Jackson GR, Owsley C, Cordle EP, Finley CD. Aging and scotopic sensitivity. *Vision Res.* 1998;38:3655–3662.
8. Jackson GR, Owsley C. Scotopic sensitivity during adulthood. *Vision Res.* 2000;40:2467–2473.
9. Owsley C, Jackson GR, White MF, Feist R, Edwards D. Delays in rod-mediated dark adaptation in early age-related maculopathy. *Ophthalmology.* 2001;108:1196–1202.
10. Curcio CA, Millican CL, Allen KA, Kalina RE. Aging of the human photoreceptor mosaic: Evidence for selective vulnerability of rods in central retina. *Invest Ophthalmol Vis Sci.* 1993;34(12):3278–3296.
11. Curcio CA, Medeiros NE, Millican CL. Photoreceptor loss in age-related macular degeneration. *Invest Ophthalmol Vis Sci.* 1996;37:1236–1249.
12. Schaal KB, Freund KB, Litts KM, Zhang Y, Messinger JD, Curcio CA. Outer retinal tubulation in advanced age-related macular degeneration: optical coherence tomographic findings correspond to histology. *Retina.* 2015;35:1339–1350.
13. Jackson GR, Owsley C, McGwin G, Jr. Aging and dark adaptation. *Vision Res.* 1999;39:3975–3982.
14. Owsley C, McGwin G, Jackson G, Kallies K, Clark M. Cone- and rod-mediated dark adaptation impairment in age-related maculopathy. *Ophthalmology*. 2007;114(9):1728–1735.
15. Flamendorf J, Agrón E, Wong WT, et al. Impairments in dark adaptation are associated with age-related macular degeneration severity and reticular pseudodrusen. *Ophthalmology.* 2015;122(10):2053–2062.
16. Laíns I, Miller JB, Park DH, et al. Structural changes associated with delayed dark adaptation in age-related macular degeneration. *Ophthalmology*. 2017;124:1340–1352.
17. Cocce KJ, Stinnett SS, Luhmann UFO, et al. Visual function metrics in early and intermediate dry age-related macular degeneration for use as clinical trial endpoints. *Am J Ophthalmol.* 2018;189:127–138.
18. Guymer RH, Tan RS, Luu CD. Comparison of visual function tests in intermediate age-related macular degeneration. *Trans Vis Sci Technol.* 2021;10:14.
19. Dimitrov PN, Robman LD, Marsamidis M, et al. Relationship between clinical macular changes and retinal function in age-related macular degeneration. *Invest Ophthalmol Vis Sci.* 2012;53:5213–5220.

20. Lott LA, Schneck ME, Haegerstrom-Portnoy G, et al. Simple vision function tests that distinguish eyes with early to intermediate age-related macular degeneration. *Ophthalmic Epidemiol*. 2021;28:93–104.

21. Sevilla MB, McGwin G, Jr, Lad EM, et al. Relating retinal morphology and function in aging and early to intermediate age-related macular degeneration subjects. *Am J Ophthalmol*. 2016;165:65–77.

22. Owsley C, McGwin G, Jr, Clark ME, et al. Delayed rod-mediated dark adaptation is a functional biomarker for incident early age-related macular degeneration. *Ophthalmology*. 2016;123:344–351.

23. Mullins RF, McGwin G, Jr, Searcey K, et al. The ARMS2 A69S polymorphism is associated with delayed rod-mediated dark adaptation in eyes at risk for incident age-related macular degeneration. *Ophthalmology*. 2018;126:591–600.

24. Hogg RE, Chakravarthy U. Visual function and dysfunction in early and late age-related maculopathy. *Prog Retin Eye Res*. 2006;25:249–276.

25. Neelam K, Nolan J, Chakravarthy U, Beatty S. Psychophysical function in age-related maculopathy. *Surv Ophthalmol*. 2009;54(2):167–210.

26. Lamb TD, Pugh ENJ. Dark adaptation and the retinoid cycle of vision. *Prog Retin Eye Res*. 2004;23:307–380.

27. Lamb TD, Pugh EN. Phototransduction, dark adaptation, and rhodopsin regeneration. *Invest Ophthalmol Vis Sci*. 2006;47:5138–5152.

28. Ramrattan RS, van der Schaft TL, Mooy CM. Morphometric analysis of Bruch's membrane, the choriocapillaries and the choroid in aging. *Invest Ophthalmol Vis Sci*. 1994;35:2857–2864.

29. Mullins RF, Johnson MN, Faidley EA, Skeie JM, Huang J. Choriocapillaris vascular dropout related to density of drusen in human eyes with early age-related macular degeneration. *Invest Ophthal Vis Sci*. 2011;52(3):1606–1612.

30. Zweifel SA, Spaide RF, Curcio CA, Malek G, Imamura Y. Reticular pseudodrusen are subretinal drusenoid deposits. *Ophthalmology*. 2010;117:303–312.

31. Curcio CA, Messinger JD, Sloan KR, McGwin G, Jr, Medeiros NE, Spaide RF. Subretinal drusenoid deposits in non-neovascular age-related macular degeneration: morphology, prevalence, topography, and biogenesis model. *Retina*. 2013;33:265–276.

32. Sparrow JR, Yoon KD, Wu Y, Yamamoto K. Interpretations of fundus autofluorescence from studies of bisretinoids of the retina. *Invest Ophthalmol Vis Sci*. 2010;51:4351–4357.

33. Spaide R, Curcio CA. Anatomic correlates to the bands seen in the outer retina by optical coherence tomography: literature review and model. *Retina*. 2011;31:1609–1619.

34. Lamb TD, Cideciyan AV, Jacobson SG, Pugh EN. Towards a molecular description of human dark adaptation. *J Physiol*. 1998;506:88P.

35. Mata NL, Radu RA, Clemmons RS, Travis GH. Isomerization and oxidation of vitamin A in cone-dominant retinas: a novel pathway for visual-pigment regeneration in daylight. *Neuron*. 2002;36:69–80.

36. Garlipp MA, Gonzalez-Fernandez F. Cone outer segment and Muller microvilli pericellular matrices provide binding domains for interphotoreceptor retinoid-binding protein (IRBP). *Exp Eye Res*. 2013;113:192–202.

37. Curcio CA, McGwin G, Jr, Sadda SR, et al. Functionally validated imaging endpoints in the Alabama study on early age-related macular degeneration 2 (ALSTAR2): design and methods. *BMC Ophthalmol*. 2020;20:196.

38. Age-Related Eye Disease Study Research Group. The Age-Related Eye Disease Study severity scale for age-related macular degeneration. AREDS Report No. 17. *Arch Ophthalmol*. 2005;123:1484–1498.

39. Ferris FLI, Wilkinson CP, Bird A, et al. Clinical classification of age-related macular degeneration. *Ophthalmology*. 2013;120:844–851.

40. Beck RW, Moke PS, Turpin AH, et al. A computerized method of visual acuity testing: adaptation of the early treatment of diabetic retinopathy study testing protocol. *Am J Ophthalmol*. 2003;135:194–205.

41. Sunness JS, Rubin GS, Applegate CA, et al. Visual function abnormalities and prognosis in eyes with age-related geographic atrophy of the macula and good visual acuity. *Ophthalmology*. 1997;104:1677–1691.

42. Arditi A. Improving the design of the letter contrast sensitivity test. *Invest Ophthalmol Vis Sci*. 2005;46(6):2225–2229.

43. Pugh ENJ. Rushton's paradox: rod dark adaptation after flash photolysis. *J Physiol*. 1975;248:413–431.

44. Jackson GR, Edwards JG. A short-duration dark adaptation protocol for assessment of age-related maculopathy. *J Ocul Biol Dis Infor*. 2008;1:7–11.

45. Leibrock CS, Reuter T, Lamb TD. Molecular basis of dark adaptation in rod photoreceptors. *Eye*. 1998;12:511–520.

translational vision science & technology

46. Ibe OC. *Fundamentals of applied probability and random processes*, 2nd ed. Cambridge, MA: Academic Press; 2014.

47. Owsley C, Jackson GR, Cideciyan AV, et al. Psychophysical evidence for rod vulnerability in age-related macular degeneration. *Invest Ophthal Vis Sci.* 2000;41:267–273.

48. Schaal KB, Legarreta AD, Grgori G, et al. Wide-field en face optical coherence tomography imaging of subretinal drusenoid deposits. *Ophthalmic Surg Lasers Imaging Retina.* 2015;46:550–559.

49. Paavo M, Lee W, Merriam JE, et al. Intraretinal correlates of reticular pseudodrusen revealed by autofluorescence and en face OCT. *Invest Ophthalmol Vis Sci.* 2017;58:4769–4777.

50. Polyak SL. *The vertebrate visual system*. Chicago: University of Chicago Press; 1957.

51. Curcio CA, Sloan KR, Kalina RE, Hendrickson AE. Human photoreceptor topography. *J Comp Neurol.* 1990;292:497–523.

52. Wu Z, Fletcher EL, Kumar H, Greferath U, Guymer RH. Reticular pseudodrusen: a critical phenotype in age-related macular degeneration. *Prog Retin Eye Res.* 2021;88:101017.

53. Zarubina AV, Neely DC, Clark ME, et al. Prevalence of subretinal drusenoid deposits in older persons with and without age-related macular degeneration, by multimodal imaging. *Ophthalmology.* 2016;123:1090–1100.

54. Owsley C, Clark ME, Huisingh CE, Curcio CA, McGwin G, Jr. Visual function in older eyes in normal macular health: association with incident early age-related macular degeneration 3 years later. *Invest Ophthalmol Vis Sci.* 2016;57:1782–1789.

55. Chung DC, McCague S, Yu Z-F, et al. Novel mobility test to assess functional vision in patients with inherited retinal dystrophies. *Clin Exp Ophthalmol.* 2018;46:247–259.